Megahertz Light Steering without Moving Parts

Adithya Pediredla[1,2], Srinivasa G. Narasimhan[2], Maysamreza Chamanzar[2], Ioannis Gkioulekas[2]
[1]Dartmouth College, [2]Carnegie Mellon University

In this supplementary material, we provide details for the renderer, additional details about the hardware setup and alignment, and additional experimental results. Along with this document, we also provide the source code of the renderer and a supplementary video.

1. Physics-based Renderer

As mentioned in the main paper, we have developed a physics-based Monte Carlo renderer to simulate the ultrasonic scanner and facilitate virtual design. Our implementation is largely based on the open-source renderer by Pediredla et al. [4]. Pediredla et al.'s work largely concerns cylindrical transducers and assumes that the refractive index field is known a priori. Contrary to that, our renderer does not require knowledge of the refractive index field analytically or numerically, as we compute the refractive index through ultrasonic wave simulation. To do so, we assume that there are no interreflections for the ultrasonic wave. Our extension can simulate multiple arbitrarily-shaped transducers, enabling us to simulate traveling-wave ultrasonic transducers. We experimented with multiple shapes and sizes of the transducers and concluded that a planar transducer is the simplest design to show proof-of-concept experiments in the main paper.

Pediredla et al.'s [4] renderer only runs on CPUs. We added GPU capability making the renderer an order of magnitude faster. We also added PyBind wrappers [1], to provide a simpler Python interface to the backend C++ code. We share the renderer and installation instructions in this supplement. Upon acceptance, we will open-source the code and the associated docker image.

The renderer can faithfully reproduce real measurements by accurately simulating sound and light physics. Therefore, the renderer can help design the hardware system through virtual experiments. We next showcase two renderer capabilities, one for system development, and another for application development.

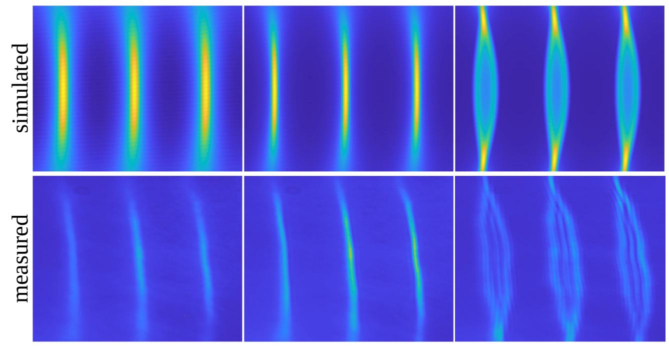

Figure 1. **Effect of voltage on line focus:** Increasing the voltage of the transducer voltage increases the power of the cylindrical lens. Therefore, for a fixed display distance, with the increase in input voltage, the light rays will initially start to focus and then defocus after the focus voltage. The defocus blur has a pointy-ended ellipsoidal shape, which our renderer faithfully reproduces.

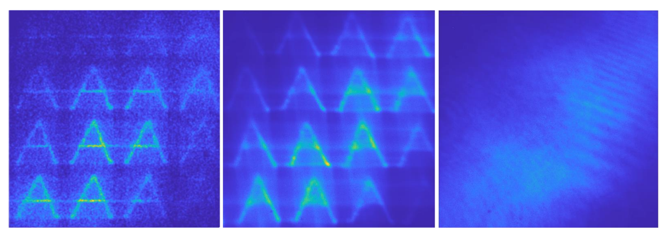

Figure 2. **Comparison of rendered and real data for dot projector application:** We compare the simulated data with real results for projecting the "A" example. We illuminated a larger portion of the ultrasonic lens to show our projector's periodic nature. The light beam is distorted due to diffraction effects from scratches on the acrylic tank. We use this beam shape for simulation. Even though our renderer does not model diffraction artifacts, we observe a good match between the simulated and measured data

System development: simulating effect of voltage settings. With the help of the renderer, we can study the effect of various system parameters, such as the shape of the transducer, the location of the transducers, and the voltage and frequency of the input waveform. In Fig. 1, we show the effect of voltage on the line projection.

At low voltages, the ultrasonically sculpted lens does not bend rays enough to focus them on the display plane. As the input voltage increases, the light rays focus better on the display plane, and defocus beyond a certain voltage. The defocus kernel has an ellipsoidal shape with pointed ends. Comparing real measurements and renderings, we observe that the renderer produces results that qualitatively match the real behavior of our ultrasonic scanner.

Component	Manufacturer
water tank	B01K8WDE4I, Amazon.com, Inc.
transducers (2)	P-25.40mm-25.40mm-2.10mm-880-WFB APC International, Ltd
amplifiers (2)	ENI A300, Bell electronics
signal generators (2)	SDG6022x, Siglent Tech.
Q-switched laser	PICOPOWER-LD-510, ALPHALAS GmbH
8-50mm C-Mount zoom lens	ArduCAM
galvo	GVS-212, Thorlabs Inc.
DAQ	USB-6343, NI Corp.
translation stages (12)	Thorlabs, Inc.
SPAD	Microphoton Devices s.r.l.
PSD	Microphoton Devices s.r.l.
picoharp	Microphoton Devices s.r.l.

Table 1. Parts required for building the prototype. Note that the scanner comprises only the water tank, transducers, and amplifiers. The remaining items are standard projector, lidar, or galvo-scanning hardware parts. The amplifiers could be replaced by standard inexpensive amplifiers that cost tens of dollars, as we only require power output of around 2 W. The estimated cost of the systems is around \$100.

Application development: simulating arbitrary dot projection. We use the renderer to simulate the dot projector application from the main paper. Unlike the result shown in the main manuscript, we illuminated a display of size approximately around $4\lambda_{us} \times 4\lambda_{us}$, to show the periodic nature of the ultrasonic scanner. In Fig. 2, we compare the simulation versus measured real data, and observe that the two closely match.

2. Additional hardware details

In the main paper, we explained the hardware prototype at a high level. In this supplement, we provide further details on how to align, calibrate, and replicate the prototype.

Table 1 lists all the components used to assemble our setup. The scanner only consists of a water tank filled with water, transducers, and amplifiers; the remaining components are required for the evaluation and proof-of-concept applications.

Fig. 3 shows the electronic circuitry we use to synchronize the transducers with the laser and the SPAD gate. In the dot projector configuration, the transducers receive phase-modulated sinusoidal input signals corresponding to the projected dot pattern. The laser receives a TTL signal with the same frequency as the transducers, and the SPAD gate receives a phase-delayed version of the laser signal. In the pulsed raster scan mode, the laser receives a TTL signal with the highest frequency that the laser can operate on. Other signals remain the same.

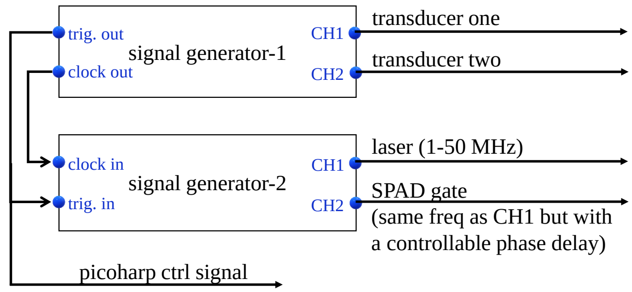

Figure 3. Electronic circuit to synchronize the transducers with laser and SPAD.

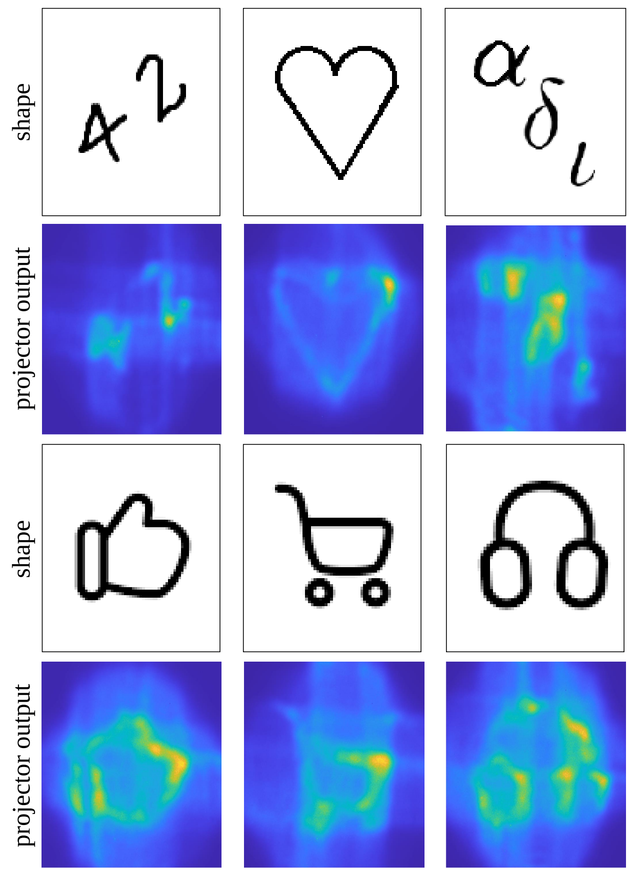

Figure 4. **Projector:** We show projector results for multiple scenes. We observe the effect of cross-shaped blur kernel on the display. This kernel could be made close to Gaussian-like by using multiple transducers placed at multiple orientations and synchronized appropriately. We can shape this blur kernel by wavefront shaping the input light wavefront.

To optically align the system, we use the following steps:

- Place the laser, SPAD, and transducers on a 3D stage.

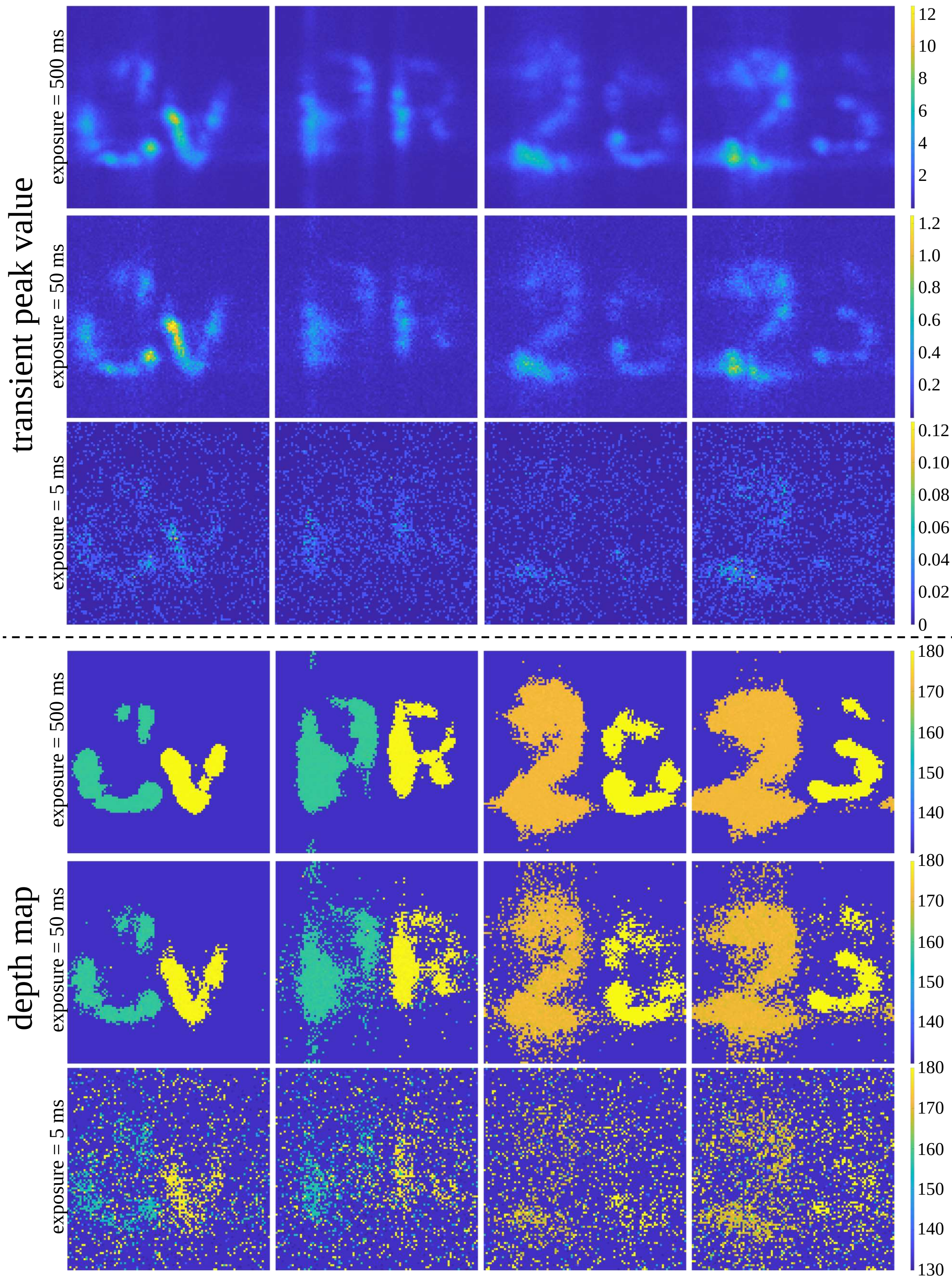

Figure 5. **Effect of exposure:** Our scanning technique could raster scan up to 50 million points, the same as the repetition rate of the laser. However, our laser is not powerful (≈1.1 mW at 50 MHz) limiting our acquisition time. We show the effect of exposure on multiple scenes showing that our technique is currently limited by the light throughput to around 50 ms even though it could theoretically scan up to 5000 frames per second at this spatial resolution. We smoothed the transient with a moving mean of size 50 bins.

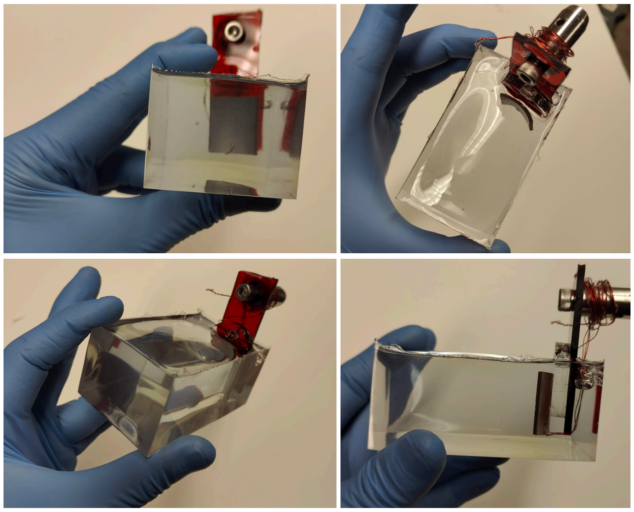

Figure 6. **Polymer medium:** Instead of water, we could use polymers to improve the form factor of the system. The speed of sound is typically higher in polymers such as epoxy, which is a desirable quality. Unfortunately, epoxy softens at higher pressure and temperature, limiting the range of voltages we could apply and observe the acousto-optic effect. Building transparent, compressible, and temperature-resistant polymers will lead to solid prototypes.

- Collocate the laser and SPAD using a beam splitter.
- Place the zoom lens between the laser and the beam splitter.
- Keep the zoom lens at the lowest focal length to diverge the beam to a large area.
- Place the filled water tank in front of the laser beam.
- Place a planar transducer in the water parallel to the beam and at 45° tilt to the bottom of the tank.
- Connect the transducer to the output of the amplifier and drive the amplifier with the signal generator.
- Drive the transducer and the laser at the same frequency (1 MHz), and the light beam will focus on a few lines. If the frequency of the transducer is changed slightly, the lines will travel at the beat frequency. The reflections of ultrasound can be visualized at this stage. Align the transducer, so the reflections do not overlap with the traveling wave.
- Place the second transducer in the water and repeat the above step. Ensure that the lines generated by both transducers are orthogonal. When both the transducers are turned on, they will form a grid of lines that intersect at dots. If the transducers are at a different distance from the zoom lens, the result will be a rectangular display. Interreflections decrease the quality of the projection.
- Increase the focal length of the zoom lens until only one focal region is illuminated.
- If the illumination still produces multiple focal regions, place an aperture after the water tank to crop and illuminate only one focal region.
- Place a retroreflective dot at the focal point.
- Run the SPAD in free running mode and spatially translate SPAD until its photon count is highest. This ensures that SPAD and laser are aligned.
- Change the SPAD to run in gated mode. Delay the gate signal to reject light backscattered by optics, by changing the phase of the input waveform to the SPAD gate (Fig. 3. signal generator-2).
- Place a 45° mirror after the aperture and redirect the beam to a galvo.
- Drive the galvo mirrors using the DAQ, similar to the previous work [2, 3].

3. Additional results

In Fig. 4, we show dot projector results for multiple scenes. we notice the effect of blur kernel and non-uniform illumination on the results.

In Fig. 5, we show the effect of exposure on the imaging and depth measurements. Even though the scanning technique is capable of scanning the depth of 50 million points per second—which translates to 5000 fps at 100×100 spatial resolution—the laser power ($\approx$ 1.1 mW at 50 MHz) limits our prototype to around 200 fps.

4. Future: solid prototype with polymers

We can replace the liquid medium in our setup with a solid medium. For example, tellurium dioxide glass is a good substitute that would also increase the speed of sound, and thus the overall quality of the system. However, working with glass is challenging. A simpler alternative is to use polymers such as epoxy. Ultrasound is $2\times$ faster in epoxy than water. In Fig. 6, we show initial attempts to make the solid prototype of our scanner with UV epoxy. Unfortunately, the epoxy softens even at low temperatures and pressure; hence, we could only observe the acousto-optic effect for low voltages. Discovering transparent polymers that can withstand high pressure is in an interesting future direction that could make our system more reliable and performant.

References

[1] Wenzel Jakob, Jason Rhinelander, and Dean Moldovan. pybind11 – seamless operability between c++11 and python, 2017. https://github.com/pybind/pybind11. 1

[2] David B Lindell, Gordon Wetzstein, and Matthew O'Toole. Wave-based non-line-of-sight imaging using fast fk migration. *ACM Transactions on Graphics (ToG)*, 38(4):1–13, 2019. 4

[3] Xiaochun Liu, Ibón Guillén, Marco La Manna, Ji Hyun Nam, Syed Azer Reza, Toan Huu Le, Adrian Jarabo, Diego Gutierrez, and Andreas Velten. Non-line-of-sight imaging using phasor-field virtual wave optics. *Nature*, 572(7771):620–623, 2019. 4

[4] Adithya Pediredla, Matteo Giuseppe Scopelliti, Srinivasa Narasimhan, Maysamreza Chamanzar, and Ioannis Gkioulekas. Optimized virtual optical waveguides enhance light throughput in scattering media. 2021. 1